Article

Not peer-reviewed version

# Screening and Network Pharmacological Analysis of Korean National Insurance-Covered Herbal Prescriptions with Therapeutic Potential for Mitigating Inflammation in Respiratory Tracts

Ga-Ram Yu , Dong-Woo Lim * , Won-Hwan Park *

Posted Date: 5 August 2024

doi: 10.20944/preprints202408.0306.v1

Keywords: long-COVID; macrophage; network pharmacology; NF-κB activation; Soshihotang (Xiao Chai Hu Tang); DEGs analysis; insurance covered herbal prescriptions

*Article*

# Screening and Network Pharmacological Analysis of Korean National Insurance-Covered Herbal Prescriptions with Therapeutic Potential for Mitigating Inflammation in Respiratory Tracts

**Ga-Ram Yu [1,2], Dong-Woo Lim [1,2,*] and Won-Hwan Park [1,*]**

[1] Department of Diagnostics, College of Korean Medicine, Dongguk University, Goyang-si 10326, Republic of Korea
[2] Institute of Korean Medicine, Dongguk University, Goyang-si 10326, Republic of Korea
* Correspondence: greatwoodong@dongguk.edu (D.-W.L.); diapwh@dongguk.ac.kr (W.-H.P.)

**Abstract:** Long COVID is a persistent symptom that appears in many COVID-19 patients, regardless of whether they are asymptomatic, mild, or severe. At least 10% worldwide are suffering from long COVID. The anti-inflammatory effect was evaluated in LPS-treated RAW264.7 cells using six Korean national insurance-covered herbal prescriptions with therapeutic potential for mitigating inflammation in the respiratory tract, and additional network pharmacology analysis was performed. Soshihotang (SST) significantly downregulated iNOS and COX2 expression, reduced the production of NO (nitric oxide) and inflammatory cytokines, such as TNFα, IL-1β, and IL-6, and inhibited IκBα phosphorylation and reduced the nuclear translocation of NF-κB in LPS-treated RAW264.7 cells. Network pharmacological analysis showed that SST was closely related to the NF-κB signaling pathway. Further study on the potential of herbal prescriptions will be needed before they can be used clinically by long COVID patients.

**Keywords:** long-COVID; macrophage; network pharmacology; NF-κB activation; Soshihotang (Xiao Chai Hu Tang); DEGs analysis; insurance covered herbal prescriptions

## 1. Introduction

The COVID-19 (Coronavirus disease 2019) pandemic affected public healthcare systems worldwide [1]. Some people who have recovered from COVID-19 or develop persistent new symptoms lasting weeks or months, called "long COVID" or "post-COVID syndrome (PCS) [2]." Generally, many infected people recovered from COVID-19 and resumed normal activities after 21 days [3]. On the other hand, 40% of infected people experience a variety of symptoms (fatigue, exertional dyspnea, insomnia, malaise, cognitive impairment, myalgia, cough, anosmia, arthralgia, chest pain, fever, tachycardia, and palpitations) after 12 weeks and are diagnosed with "long COVID." Long COVID patients show the persistent deregulation of a wide range of cytokines long after infection [4–6]. In particular, the levels of some inflammatory cytokines, including TNF-α, IL-1β, and IL-6, remain at significantly high levels in patients with sequelae [7]. Sustained immune activation has been suggested to be associated with ongoing symptoms following COVID-19 [8].

Macrophages are the most important cells of the innate immune system and form the first line of defense against microbes, triggering innate immunity by recognizing pathogen-associated molecular patterns [9]. Lipopolysaccharide (LPS), the primary pathogenic factor of acute lung injury, is a highly acylated saccharolipid located on the outer leaflet of the outer membrane of Gram-negative bacteria that acts as an effective initiator of local acute inflammation [10,11]. Macrophages involved in the inflammatory process produce large amounts of nitric oxide (NO) and pro-inflammatory cytokines such as TNFα, IL-1β, and IL-6 [12]. NO synthesized by inducible nitric oxide synthase

 doi:10.20944/preprints202408.0306.v1



(iNOS) plays an important role in the immune and nervous systems [13]. iNOS is expressed in various cell types, including macrophages, hepatocytes, and astrocytes, and induced in response to various factors, such as LPS and pro-inflammatory cytokines [14]. Prostaglandins (PGs) are the metabolites of cyclooxygenase-2 (COX-2), which play a critical role during inflammatory responses [15]. iNOS and COX2 play essential roles in the pathophysiology of acute lung injury (ALI) [16]. In addition, the activation of NF-κB (nuclear factor kappa-light-chain-enhancer of activated B cells) plays an important role in developing acute lung injury [17]. NF-κB is sequestered by inhibitors of NF-κB alpha (IκBα) in the cytoplasm. The activation of NF-κB by inflammatory stimulants occurs via the phosphorylation of IκBα. Phosphorylated IκBα is dissociated from the p65/IκBα complex, and NF-κB translocates into the nucleus, where it regulates several genes important for immunity, including iNOS, COX-2, and specific cytokines/chemokines [18]. The nuclear regulatory factor NF-κB is activated in the lungs of patients with acute respiratory distress syndrome (ARDS) and may contribute to the increased expression of pro-inflammatory cytokines/chemokines and other pro-inflammatory mediators such as ROS and NO [19–21].

Among the 56 types of herbal medicine prescriptions covered by the National Health Insurance in South Korea, this study selected prescriptions that can potentially improve respiratory diseases or symptoms. Bulhwangeumjeonggisan (BGS), Samsoeum (SSE), Saengmaeksan (SMS), Soshihotang (SST), Socheongryongtang (SCT), and Haengsotang (HST) are centuries-old traditional herbal medicine prescriptions related to respiratory diseases and symptoms, and the extracts are currently commercialized in clinics. Herbal medicine prescriptions that effectively treat respiratory-related inflammatory diseases can be discovered among insurance-covered herbal medicine prescriptions, expanding their indications with uncovered respiratory diseases or symptoms.

Network pharmacology (NP) approaches provide a new methodology to understand and predict drug combinations for treating various diseases [22]. The traditional Chinese medicine systems pharmacology database and analysis platform (TCMSP) was built based on the framework of systems pharmacology for herbal medicines [23]. The platform includes 499 Chinese herbs, 29,384 ingredients, 3,311 targets, and 837 associated diseases [24]. This study used a bioinformatics methodology combined with network pharmacological analysis to investigate the pharmacological impact of potent herbal prescriptions against the inflammatory to assess its potential to inflammatory respiratory conditions.

In this study, six prescriptions sub-classified to treat respiratory diseases were evaluated in an inflammation-induced macrophage model, and the components and target information of the possible prescription were analyzed using the latest network pharmacology technique and online pharmacological database.

## 2. Materials and Methods

### *2.1. Prescriptions and Chemicals*

Six TKM (Traditional Korean Medicine) prescriptions were purchased from Kyungbang Pharmaceuticals (Incheon, South Korea): Bulhwangeumjeonggisan (BGS), Samsoeum (SSE), Saengmaeksan (SMS), Soshihotang (SST), Socheongryongtang (SCT), and Haengsotang(HST) (The ingredients in the prescription are shown in a Supplementary Table S1). Dulbecco's Modified Eagle's Medium (DMEM) was obtained from Hyclone (Logan, UT, USA), and FBS (Fetal bovine serum) and Penicillin/Streptomycin solution were acquired from Invitrogen (Carlsbad, CA, USA). LPS (Lipopolysaccharide) was supplied by Sigma Chemicals (St. Louis, MO, USA), and the EZ-Cytox assay kit was procured from Daeil Lab Service (Chungcheongkuk-do, South Korea). RIPA buffer (radioimmunoprecipitation assay buffer) and BCA (Bicinchoninic Acid) protein assay kit were purchased from Thermo Fisher Scientific (Waltham, MA, USA). The protease and phosphatase inhibitor cocktail was obtained from GenDEPOT (Katy, TX, USA). The primary antibodies for iNOS (Inducible nitric oxide synthase), COX2 (Cyclooxygenase-2), Lamin B, β-actin, and horseradish peroxidase (HRP)-conjugated secondary antibody were supplied by Santa Cruz (Dallas, TX, USA). The phosphorylated or non-phosphorylated primary antibodies of IκBα and NF-κB were obtained from Cell Signaling Technology (Berkeley, CA, USA), which also supplied secondary antibodies. The

 doi:10.20944/preprints202408.0306.v1



nuclear and cytoplasmic extraction reagents kit was purchased from Thermo Fisher Scientific (Rockford, IL, USA) and used to separate nuclear and cytosolic proteins. The oligonucleotide primers (COX2, TNFα, IL-6, and IL-1β) used for real-time qPCR were supplied by Macrogen (Seoul, South Korea). Quantikine mouse ELISA kits (TNFα, IL-6, IL-1β) were purchased from R&D Systems (Minneapolis, MN, USA).

*2.2. Cell Culture and Treatment*

RAW264.7 cells (a mouse macrophage cell line) were purchased from the Korea Cell Line Bank (KCLB, Seoul, South Korea). The cells were cultured in DMEM, supplemented with 10% FBS and 100 U/mL penicillin-streptomycin. Cells were incubated at 37°C in a humidified 5% $CO_2$ atmosphere and maintained at ~70% confluence before being used in the experiments [25]. The cells were co-treated with LPS (1 μg/mL) and the samples for 6 h (for real-time PCR and immunofluorescence microscopy) or 12–24h (Nitrite determination and Western blot).

*2.2. Cell Viability Assay*

The cell viability of the RAW264.7 cells was determined using an EZ-Cytox assay kit (Daeil Lab, Seoul, South Korea) according to the manufacturer's instructions. Briefly, the cells were seeded in 96-well plates in DMEM at a density of $3 \times 10^3$ cells per well and then incubated with various concentrations of samples at 37°C in a humidified atmosphere containing 5% $CO_2$ for 24 h when the medium was replaced with FBS-free DMEM, treated with EZ-Cytox reagent for 30 min. The optical densities (ODs) of the reactants were measured at 450 nm using a microplate spectrophotometer (Versamax, Molecular Devices, USA) [26].

*2.3. Nitrite Determination*

Griess reagent was used to examine the effects of the samples on LPS-induced nitrite levels. Briefly, RAW264.7 cells ($3 \times 10^4$ cells/well) were seeded in six-well plates for nitric oxide (NO) measurements and incubated at 37°C in a humidified atmosphere containing 5% $CO_2$. At 24 h after seeding, the cells were co-treated with LPS (1 μg/mL) and samples for 24 h. The supernatants were collected, mixed with Griess reagent (a mixture of 0.1% N-(1-naphthyl) ethylenediamine (NED) and 1% sulfanilamide dissolved in 5% phosphoric acid) and incubated for 15 min. The ODs were measured at 540 nm using a microplate spectrophotometer. The nitrite concentrations were calculated using a standard curve [27].

*2.4. Western Blot*

The protein levels of inflammatory markers were determined by Western blot. Briefly, the cells were washed with DPBS (Dulbecco's phosphate buffered saline), and the whole proteins were then isolated using ice-cold RIPA buffer containing protease and phosphatase inhibitor cocktail. The protein concentrations in the cell lysates were determined using a commercial BCA kit. The protein lysates (35 μg) were loaded into 7.5% or 10% SDS-PAGE gels, electrophoresed, and transferred to PVDF membranes at 100 V for 60 min using the Mini transblot electrophoretic transfer cell device (Bio-Rad, Hercules, CA, USA). The membranes were then blocked in TBS/T (TBS containing 0.1% Tween 20) containing 5% BSA for 2 h at room temperature, and the blots were incubated with the primary antibody (diluted at 1:1000 in TBS/T containing 3% BSA) overnight at 4°C with gentle shaking and washed. Subsequently, the membranes were incubated with the secondary antibody (diluted at 1:3000 in TBS/T containing 1% BSA) for 2 h. Chemiluminescent blots were developed using an enhanced chemiluminescence (ECL) buffer (Super Signal West Pico, Thermo Fisher Scientific), and blots were detected using a western blot imaging system (Fusion Solo, Vilber Lourmat, Collegien, France) [28].

 doi:10.20944/preprints202408.0306.v1



*2.5. Immunofluorescence Assay*

The nuclear translocation of NF-κB was followed by cultivating the cells on Lab-Tek II chamber slides (Nalge Nunc, IL, USA), using a slight modification of the methodology described elsewhere. Briefly, the cells were fixed in 4% formaldehyde for 5 min, permeabilized with 0.1% Triton X-100 for 10 min at room temperature, blocked with 3% BSA for 1 h at room temperature, and labeled with 2 μg/mL of NF-κB primary antibody diluted in 1% BSA overnight at 4℃. NF-κB in the cytoplasm and nuclei was detected by treating the cells with PBS containing 2 μg/mL of FITC for 1 h at room temperature. Nuclei were stained using a mounting medium containing DAPI (Vector Laboratories, CA, USA) [29]. The images were captured under a fluorescence microscope (BX50, Olympus, Japan).

*2.6. Quantitative Real-Time Polymerase Chain Reaction*

qPCR was used to measure the mRNA expression levels of the pro-inflammatory mediators associated genes. The cells were seeded in 60 mm culture plates for 24 h and co-treated with LPS (1 μg/mL) under the same conditions described above. The total mRNA was isolated using the Trizol reagent (Invitrogen, Carlsbad, CA, USA) according to the manufacturer's instructions. Briefly, isolated mRNA was subjected to cDNA synthesis using the AccuPower RT Premix kit (Bioneer, Daejeon, South Korea) and oligo deoxythymine (dt) 18 primers (Invitrogen, Carlsbad, CA, USA). Primer-specific binding cDNA was amplified using a Light Cycler 480 PCR system (Roche, Basel, Switzerland). The PCR mix contained 10 μL of SYBR green master mixture (Roche, Switzerland), 8 μL of ultrapure water, 1 pmol/μL of gene primer, and 1 μL of template cDNA. Amplification was performed using the following schedule: initial denaturation at 95°C for 10 min, followed by 45 cycles of denaturation at 95°C for 10 s, annealing at 50–60°C for 20 s, and extension at 72°C for 20 s. The following primers were used: COX2 forward, 5′- GCG ACA TAC TCA AGC AGG AGC A -3′, reverse, 5′- AGT GGT AAC CGC TCA GGT GTT G -3′; TNFα forward, 5′- AAG CCT GTA GCC CAC GTC GTA -3′, reverse, 5′- GGC ACCA CTA GTT GGT TGT CTT TG -3′; IL-1β forward, 5′- CTG AAC TCA ACT GTG AAA TGC CA -3′, reverse, 5′- AAA GGT TTG GAA GCA GCC CT -3′; IL-6 forward, 5′- CCA CTT CAC AAG TCG GAG GCT TA -3′, reverse, 5′- GCA AGT GCA TCA TCG TTG TTC ATA C -3′; β-actin forward, 5′- GCA AGT GCT TCT AGG CGG AC -3′, reverse, 5′- AAG AAA GGG TGT AAA ACG CAG C -3′. β-actin was used as the internal control, and the results were normalized by dividing the gene threshold cycle values (Ct value) by that of β-actin. All data were acquired using Roche LightCycler 480 software (Roche Applied Science, USA) [30].

*2.7. ELISA Analysis*

Concentrations of inflammatory cytokines, i.e., TNFα, IL-1β, and IL-6, in the cell culture supernatants were quantified using Quantikine mouse ELISA kits. Briefly, the cells ($3 \times 10^5$ cells/well) were seeded in the six-well plates for ELISA and incubated at 37°C in a humidified atmosphere containing 5% $CO_2$. Twenty-four hours after seeding, the cells were co-treated with LPS (1 μg/mL) and samples for 24 h. The culture media were then collected, and the TNFα, IL-1β, and IL-6 concentrations were measured according to the manufacturer's instructions. The optical densities were measured at 450 nm using a microplate spectrophotometer [31].

*2.8. Acquisition of Potential Active Ingredients and Targets of SST and Isolating Long-Covid DEGs from Online Database*

The SST used in this study consisted of seven different medicinal herbs: Bupleuri Radix (BR), Ginseng Radix (GR), Glycyrrhizae Radix (GLR), Jujubae Fructus (JF), Pinellae Tuber (PT), Scutellariae Radix (SR), and Zingiberis Rhizoma (ZR). The traditional Chinese medicine systems pharmacology database and analysis platform (TCMSP, https://old.tcmsp-e.com/tcmsp.php) was used as a repository to collect information on the ingredients of SST. Potential bioactive ingredients in each herb were screened using the ADME (absorption, distribution, metabolism, and excretion)-related pharmacokinetic properties, especially for drug-likeness (DL, ≥0.18) and oral bioavailability (OB, ≥30%). Targets related to long COVID were obtained using the GEO database

 doi:10.20944/preprints202408.0306.v1



(https://www.ncbi.nlm.nih.gov/geo/). The search strategy included "long COVID," "Homo sapiens," and "Expression profiling by high throughput sequencing." Based on the above retrieval strategy, the gene expression profiles selected for analysis from the GEO database was GSE251849 [32]. The microarray data of differentially expressed mRNA in the long COVID between the normal group (five healthy females) and the long COVID (five unhealthy females) were obtained from the GEO database. The distributional results of the target and ingredients from herbs were presented as Venn diagrams using the Statistical Utility for Microarray and Omics data (SUMO) software downloaded from website (https://angiogenesis.dkfz.de/oncoexpress/software/sumo/).

### *2.9. Protein-Protein Interaction (PPI) Network Construction*

All targets of the seven herbs ingredients were arranged as lists and uploaded to the STRING database (https://string-db.org/) to construct a PPI network with an interaction score of medium confidence (0.400). The DEGs that overlapped with the SST target genes were further separated by up- and down-regulated DEGs. The PPI network connectivity of up- and down-regulated DEGs were exported as images for further analysis [33].

### *2.10. Gene Ontology (GO) Enrichment and KEGG Pathway Analysis*

DAVID database platform (https://david.ncifcrf.gov) was used to collect GO (Gene ontology) analysis and KEGG (Kyoto Encyclopedia of Genes and Genomes) data to study the biological function of potential targets. A list of all key genes was uploaded, and the identifier was set as the "official gene symbol." Annotations of the key genes were identified in the KEGG pathway and GO analysis. GO analysis was used to screen biological processes (BP). KEGG enrichment analysis can find important signaling pathways involved in biological processes. The top 20 results with the lowest P-values in each category were visualized as a bubble chart containing P-values, gene counts, and gene ratios. Bubble plots were produced using the R studio software and the 'ggplot2' package with a public R script modified for the study [34].

## 3. Results

### *3.1. Effects of Prescriptions on RAW264.7 Cell Viability*

RAW264.7 macrophages were incubated with various concentrations of six TKM prescriptions for 24 h. Macrophages showed no significant decrease in viability at most sample concentrations of <100 μg/mL (86.93%, 90.94%, 84.90%, 88.29, 88.29, and 100.04% at 100 μg/mL). On the other hand, HST did not have any significant cytotoxic effects. Subsequent experiments were conducted using six TKM prescriptions at 50 and 100 μg/mL (Figure 1A). The effects of six TKM prescriptions on iNOS and COX2 expression in LPS-stimulated macrophages were examined. Subsequently, this study investigated the effects of six TKM prescriptions on LPS-induced NO production in RAW264.7 macrophages. The NO levels in the medium significantly increased by LPS at 1 μg/mL for 24 h. Among the six TKM prescriptions, SST reduced NO production significantly. SST at 100 μg/mL maximally decreased NO levels from 17.04 to 13.02 μM in RAW264.7 cells (Figure 1B). SST significantly inhibited the LPS-induced iNOS and COX2 protein levels in the macrophages (Figure 1C).

### *3.2. Effects of Six TKM Prescriptions on the Nuclear Translocation of NF-κB in LPS-Stimulated Macrophages*

The effects of six TKM prescriptions on phosphorylation of IκBα were investigated because phosphorylation of IκBα was the critical step in NF-κB activation. Compared with the unstimulated macrophages, the p-IκBα protein content increased rapidly by approximately two-fold after 6 h of LPS stimulation, which suggested the activation of NF-κB protein. Western blot showed that BGS, SSE, SMS, SST, and SCT inhibited the LPS-induced phosphorylation of IκBα (Figure 2A). SSE, SMS, SST, and HST blocked NF-κB translocation to the nucleus (Figure 2B). The immunofluorescence assay images indicated that SST reduced the nuclear translocation of NF-κB (Figure 2C).

 doi:10.20944/preprints202408.0306.v1



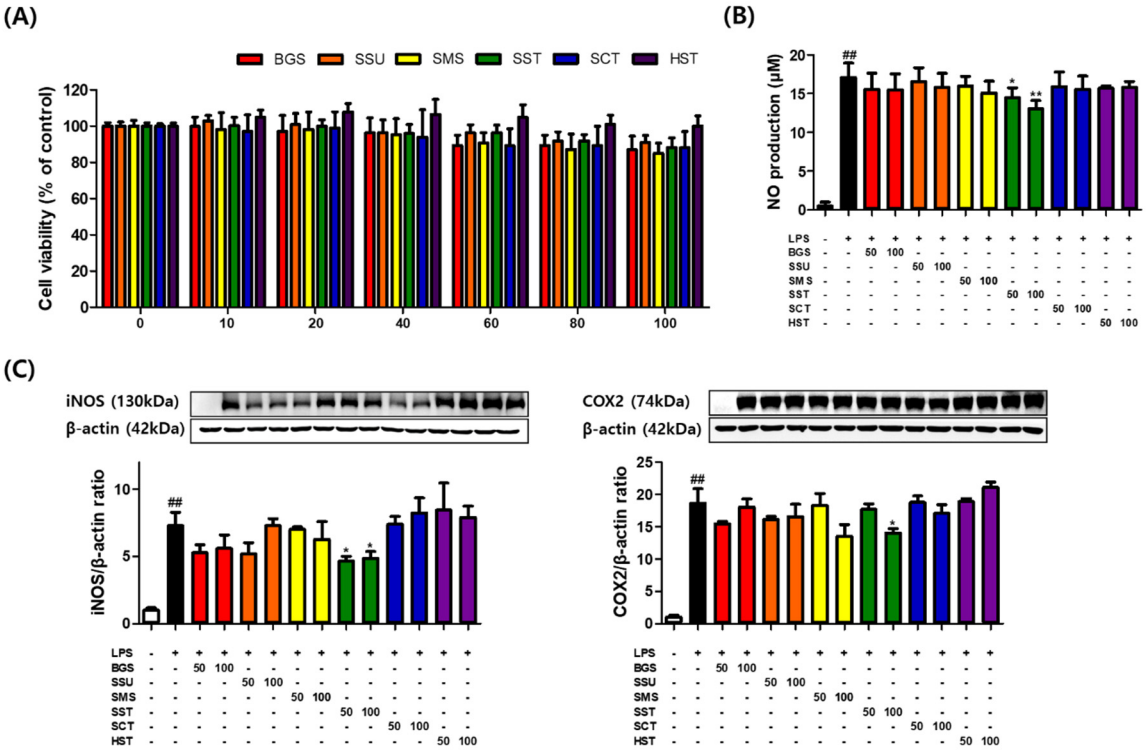


**Figure 1.** SST decreased iNOS and COX2 expression in LPS-treated macrophages. RAW264.7 macrophages incubated with the absence or presence of LPS (1 μg/mL) with six prescriptions for 24 h. (A) RAW264.7 cells were treated with various concentrations (0–100 μg/mL) of BGS, SSE, SMS, SST, SCT, and HST for 24 h. The results are presented as means ± SDs of the percentages determined by three independent experiments versus the non-treated controls. (B, C) RAW264.7 cells were co-treated with each sample and LPS (1 μg/mL) for 24 h. NO concentrations were measured using a Griess reagent. Western blot analysis shows the effect on the relative iNOS and COX-2 protein levels. The band intensities were measured by densitometry and normalized versus the intensities of the total forms and β-actin. The results are presented as the means ± SDs of three independent experiments. ##P < 0.01 versus LPS-treated controls, and *P < 0.05, **P < 0.01 versus LPS-treated RAW264.7 cells.

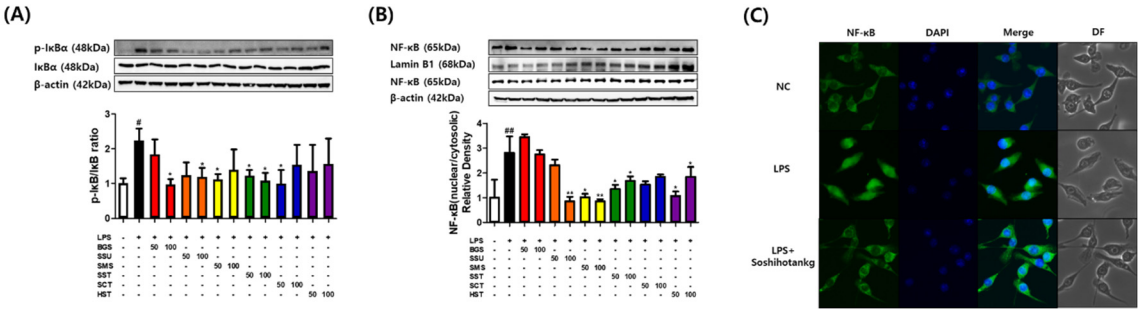


**Figure 2.** SST suppressed nuclear translocation of NF-κB in LPS-treated macrophages. RAW264.7 macrophages incubated in the absence or presence of LPS (1 μg/mL) with six prescriptions for 6 h. (A, B) Relative phosphorylation of IκB and the nuclear translocation of NF-κB as determined by western blot. (C) Immunofluorescence microscopy images. The results are presented as the means ± SDs of three independent experiments. #P < 0.05, ##P < 0.01 versus LPS-treated controls, and *P < 0.05, **P < 0.01 versus LPS-treated RAW264.7 cells.

 doi:10.20944/preprints202408.0306.v1



### *3.3. Effects of Six TKM Prescriptions on Pro-Inflammatory Cytokines Levels in LPS-Stimulated Macrophages*

qPCR and ELISA were conducted to examine the effects of six TKM prescriptions on pro-inflammatory cytokine production. The qPCR results showed that six TKM prescriptions significantly inhibited the LPS-induced expression of the TNFα gene. On the other hand, IL-6 and IL-1β expression decreased significantly in SMS, SST, SCT, and HST (Figure 3A). The ELISA results showed that a decrease in pro-inflammatory cytokines was confirmed in some prescriptions, but a strong decrease was observed in SST (Figure 3B).

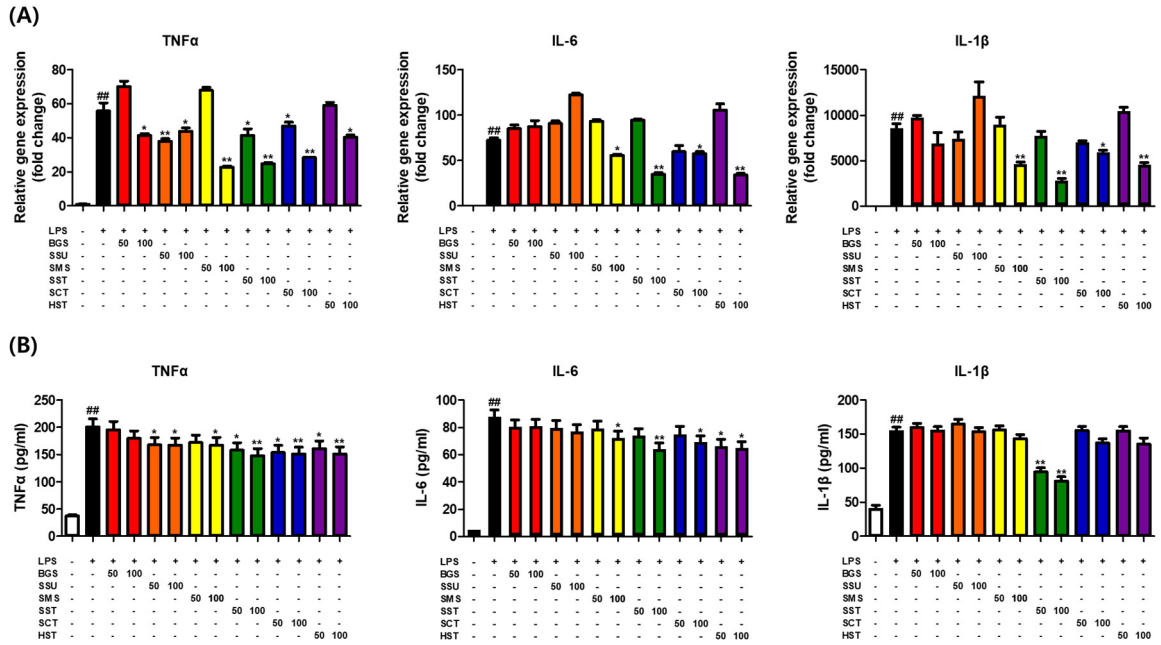


**Figure 3.** SST reduced pro-inflammatory cytokine levels in LPS-treated macrophages.

### *3.4. Active Compound Screening and Key Targets of SST*

According to the TCMSP database, 193 ingredients from the seven herbs in SST, respectively, met the OB and DL criteria (Figure 4A). Two hundred and seventy-eight potential targets of active ingredients from the seven herbs were obtained, and a Venn diagram showed all the targets (Figure 4B). Among these herbs, Glycyrrhizae Radix has the largest list of active compounds (92) and their known targets (229) for the reported ingredients. Ginseng Radix, which has been studied widely for its saponin-based bioactivity, has been shown to interact with 114 targets.

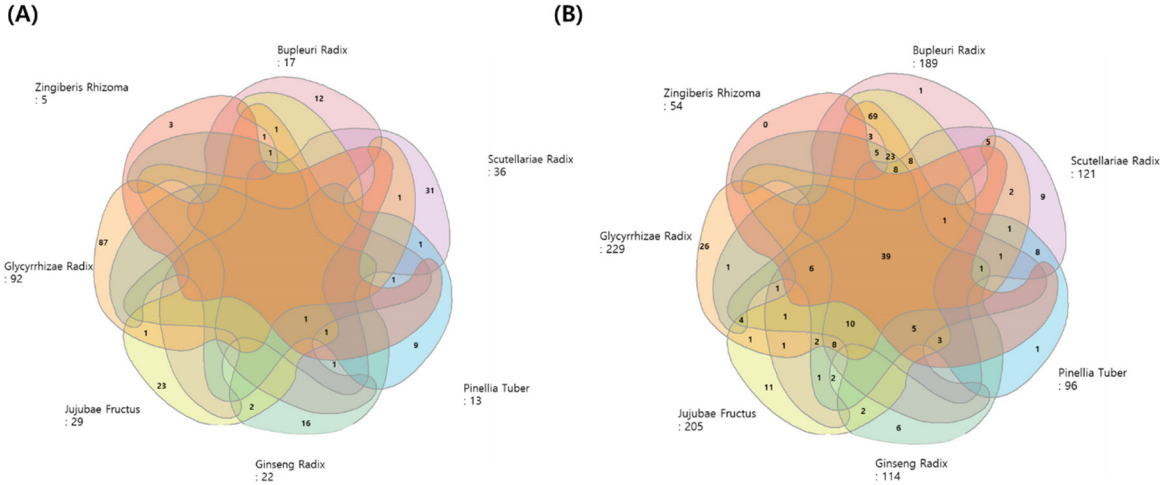

 doi:10.20944/preprints202408.0306.v1



**Figure 4.** Venn diagrams of the compounds and target genes from the seven herbs of SST. (A) Venn diagram showing the distribution of potent active compounds in the seven herbs (B) Venn diagram showing all the targets of seven herbs related to long COVID-19.

### *3.5. Identification of COVID-19 Associated-Targets*

The DEGs between long-COVID female and healthy female individuals were screened with the criteria of gene expression fold change and its p-value ($|\log2\ FC|>1$ and $P<0.05$). Transcriptomic analysis of peripheral blood mononuclear cells in the GEO database (GSE251849) contained five samples from healthy female individuals and five samples from long COVID-19, which identified 750 differentially expressed genes related to long COVID-19. Figure 5A presents a volcano plot of the distribution of the DEGs datasets, and Supplementary Figure S1 shows the quality assessment results of the datasets. The 750 long-COVID-19-related target genes were matched with the potential targets of SST. The intersection of the active compound targets of SST and disease targets of long-COVID-19 included 20 common targets (Figure 5B). The full PPI network comprised 20 key targets as nodes and 59 interactions between targets as edges (Figure 6). Cluster 1 consisted of upregulated targets with 13 key targets as nodes and 32 interactions between targets as edges.

### *3.6. Identification of COVID-19 Associated-Targets*

The 20 key target genes were uploaded into the DAVID database, and 20 results for the KEGG pathway and GO enrichment analysis were obtained using the smallest false discovery rate P-values (Figure 7). Of the 20 pathways, 13 were human disease pathways, and seven were signaling pathways. Of the seven signaling pathways, three pathways were involved in the immune system. Among the signaling pathways, the TNF$\alpha$, IL-17, and NF-κB signaling pathways were most significantly enriched (Figure 7).

RAW264.7 macrophages incubated in the absence or presence of LPS (1 μg/mL) with six prescriptions for 12 h or 24 h. (A) Relative expression of TNF$\alpha$, IL-6, and IL-1β as determined by qPCR. (B) Relative expression of TNF$\alpha$, IL-6, and IL-1β as determined by ELISA. The results are presented as the means ± SDs of three independent experiments. #$P < 0.05$ versus LPS-treated controls, and *$P < 0.05$, **$P < 0.01$ versus LPS-treated RAW264.7 cells.

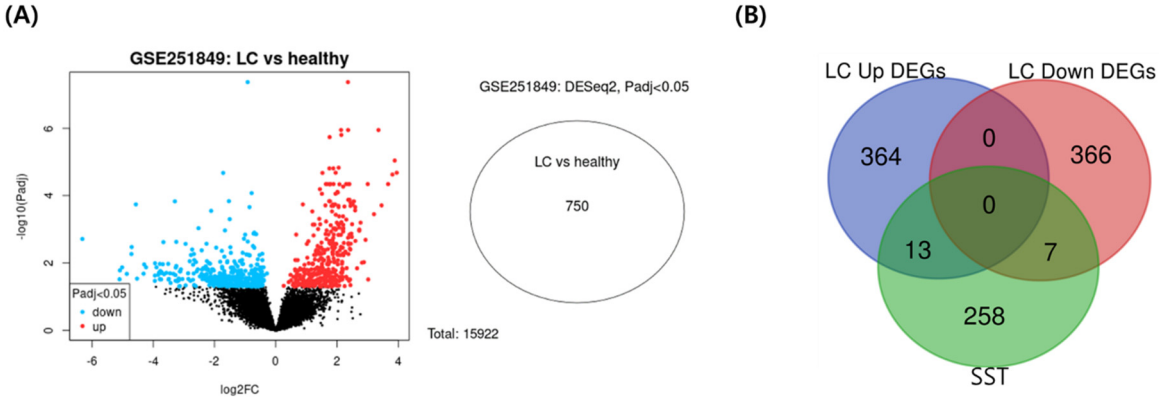


**Figure 5.** (A) Volcano plot analysis was performed for the GSE251849 differentially expressed proteins. (B) Venn diagram showing the functional targets of upregulated DEGs and down-regulated DEGs.

Preprints.org (www.preprints.org) | NOT PEER-REVIEWED | Posted: 5 August 2024 doi:10.20944/preprints202408.0306.v1



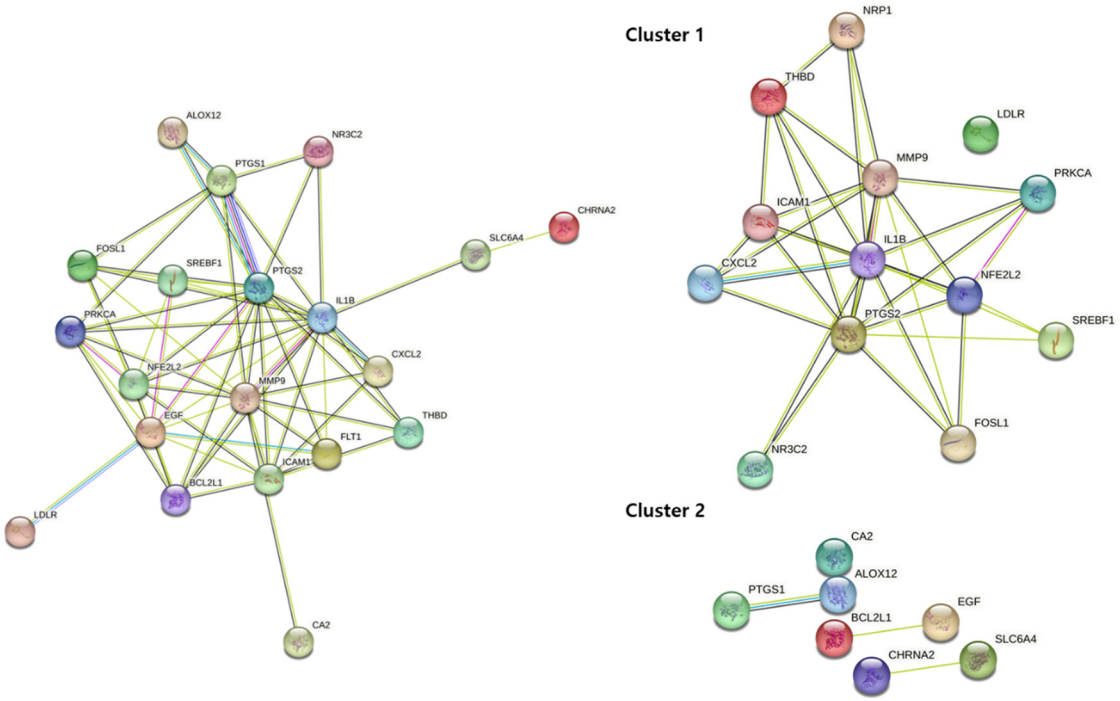


**Figure 6.** Clustering of the PPI network and enrichment analysis of long COVID-19-related up and down-regulated DEGs overlapping with the SST. The total PPI network and functional clusters of up(cluster 1) and down(cluster 2)-regulated DEGs.

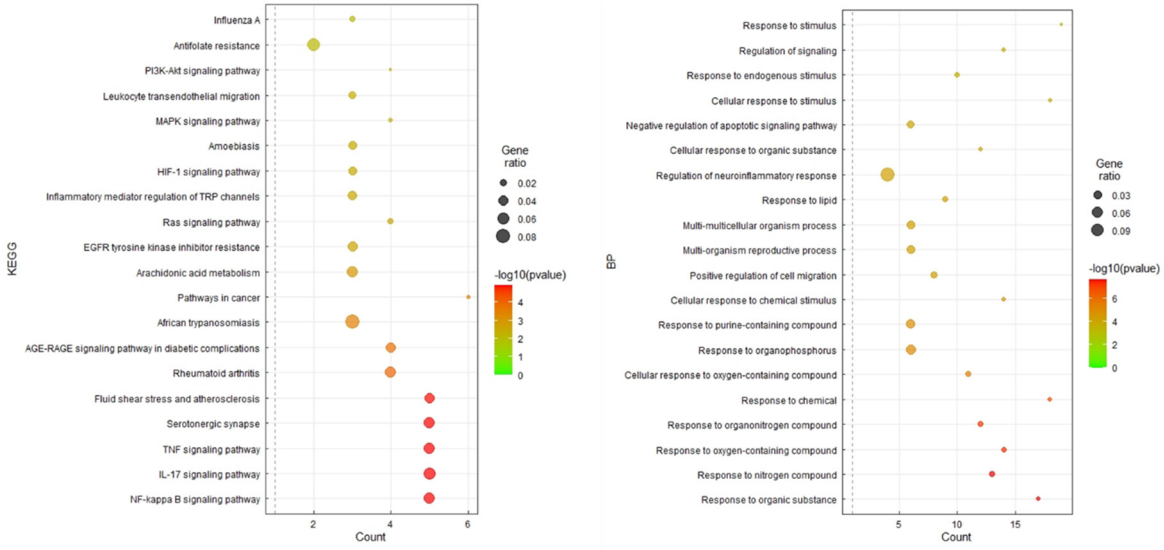


**Figure 7.** Bubble plot image of enrichment analysis (KEGG pathway and BP terms) from all targets in the seven herbs. BP term (right) and KEGG pathways (left). PPI protein–protein interaction, DEGs differentially expressed genes, BP biological process, KEGG Kyoto encyclopedia of genes and genomes.

## 4. Discussion

This study examined the fundamental anti-inflammatory effects of herbal prescriptions among herbal medicine prescriptions covered by national health insurance on long-covid-related symptoms. Lim et al. rearranged 56 insurance-covered herbal prescriptions into major disease code classifications using their annotated disease/symptom indications for further investigations [35]. A group of herbal prescriptions considered suitable for the long-lasting inflammatory status in the

 doi:10.20944/preprints202408.0306.v1



respiratory system were selected according to their clinical property (deficiency status in traditional medicine) to treat chronic inflammatory status caused by macrophages. Among the six respiratory-related prescriptions, SST decreased iNOS and COX2 expression significantly and reduced pro-inflammatory cytokine production (TNF$\alpha$, IL-6, and IL-1$\beta$) in LPS-treated RAW264.7 cells. SST reduced NO production significantly by decreasing iNOS expression. Reducing NO production is a crucial strategy for terminating the COVID-19-related inflammatory status [36]. During the inflammatory process, IL-6 and IL- 1$\beta$ may enhance the inflammatory response by promoting the recruitment and activation of neutrophils [37]. Pro-inflammatory cytokines production induced by LPS is mediated via NF-κB translocation. The phosphorylation of IκB$\alpha$ proteins induces the disassembly of the p65/IκB$\alpha$ complex, which initiates NF-κB activation in the cytoplasm and translocation to the nucleus [38]. SSE, SMS, and SST inhibited the phosphorylation of IκB$\alpha$ and reduced nuclear translocation of NF-κB. Among the six prescriptions, SSE, SMS, and SST contain ginseng. Ginseng contains more than 150 natural ginsenosides and saponins and has been reported to play various pharmacological roles in diseases, including inflammatory diseases, autoimmune diseases, cardiovascular diseases, metabolic diseases, and cancer [39,40]. Ginsenosides in ginseng modulate immunity through different pathways and may promote repair rather than completely suppress immunity [41]. According to Korean medicine, the ginseng rhizome has various effects, including strengthening vitality, invigorating the spleen, replenishing qi (氣), stimulating body fluids, and calming the nerves [42]. In terms of pharmacology, ginsenoside Rb1 (Ginseng Radix), saikosaponin B2 (Bupleuri Radix), baicalin (Scutellariae Radix), and glycyrrhizin (Glycyrrhizae Radix) in SST has a strong anti-inflammatory effect by regulating toll-like receptor 4 dimerization and NF-κB/MAPK signaling pathway [43,44].

SST, a well-known Oriental herbal prescription (Xiao Chai Hu Tang in Chinese) composed of seven herbs, has been traditionally prescribed to treat viral infections and chronic metabolic disorders in Asia [45]. Interestingly, a recent scope review recommended that SST be administered to COVID-19 patients in various East-Asian countries during the early phase of the pandemic in 2020 [46]. The efficacy of a prescription is based on the complex effects of mixed compounds. Therefore, it is necessary to understand the complex interactions between multiple compounds in herbal medicine and their multiple targets. Network pharmacology approaches can be used to interpret the complex activity mechanisms of multiple compounds and predict their pharmacological activity [47,48]. Compounds and targets for Bupleuri Radix (BR), Ginseng Radix (GR), Glycyrrhizae Radix (GLR), Jujubae Fructus (JF), Pinellae Tuber (PT), and Scutellariae Radix (SR) and Zingiber Rhizome (ZR) were obtained from the TCMSP database. SST contains 163 compounds (BR: 13, GR: 17, GLR: 88, JF: 19, PT: 12, and SR: 32), which have 278 targets (BR: 189, GR: 114, GLR: 229, JF: 205, PT: 96, and SR: 121). The DEGs deduced from long COVID patients compared to the normal group and long COVID were obtained from the GEO database. The pharmacological targets of herbs constituting SST overlapped with 20 of the DEGs. Through PPI analysis, 13 upregulated genes (NRP1, THBD, LDLR, MMP9, ICAM1, PRKCA, IL-1B, CXCL2, PTGS2, NFE2L2, SREBF1, FOSL1, and NR3C2) and seven down-regulated genes (CA2, PTGS1, ALOX12, BCL2L1, EGF, CHRNA2, and SLC6A4) were identified. The NF-κB, TNF$\alpha$, and IL-17 pathways were found to be related by KEGG enrichment analysis. SST showed the best performance among six insurance-covered TKM prescriptions. Therefore, SST has a high potential to attenuate inflammatory status caused by respiratory-infectious.

## 5. Conclusions

This study screened for proper herbal prescriptions covered by national health insurance to treat the long COVID symptoms of sustaining inflammation in the respiratory systems. The modulatory effect of six herbal prescriptions classified in a previous study was tested. Among them, SST has significant anti-inflammatory effects by alleviating the NF-κB signaling pathway as deduced by network pharmacologic analysis. Further study on the potential of the herbal prescription for clinical use on long-COVID patients is required.

 doi:10.20944/preprints202408.0306.v1



**Supplementary Materials:** The following supporting information can be downloaded at the website of this paper posted on Preprints.org, Figure S1: Quality assessment results of the datasets; Table S1: Ingredients in the prescription.

**Author Contributions:** For research articles with several authors, a short paragraph specifying their individual contributions must be provided. The following statements should be used "Conceptualization, G.-R.Y; methodology, G.-R.Y; software, D.-W.L; validation, D.-W.L; data curation, D.-W.L; writing—original draft preparation, G.-R.Y; writing—review and editing, D.-W.L; supervision, D.-W.L and W.-H.P; funding acquisition, G.-R.Y and D.-W.L; All authors have read and agreed to the published version of the manuscript."

**Funding:** This work was supported by the Basic Science Research Program of the Korean National Research Foundation funded by the Ministry of Education (Grant no. 2022R1A6A3A01087626).

**Institutional Review Board Statement:** Not applicate

**Informed Consent Statement:** Not applicate

**Data Availability Statement:** Not applicate

**Acknowledgments:** This work was supported by the Basic Science Research Program of the Korean National Research Foundation, funded by the Ministry of Education (Grant no. 2022R1A6A3A01087626).

**Conflicts of Interest:** The authors declare no conflict of interest

## References

1. Ali, S.A.; Baloch, M.; Ahmed, N.; Ali, A.A.; Iqbal, A. The outbreak of Coronavirus Disease 2019 (COVID-19)—An emerging global health threat. *Journal of infection and public health* **2020**, *13*, 644-646.
2. Yong, S.J.; Liu, S. Proposed subtypes of post-COVID-19 syndrome (or long-COVID) and their respective potential therapies. *Reviews in medical virology* **2022**, *32*, e2315.
3. Raveendran, A.; Jayadevan, R.; Sashidharan, S. Long COVID: an overview. *Diabetes & Metabolic Syndrome: Clinical Research & Reviews* **2021**, *15*, 869-875.
4. Davis, H.E.; McCorkell, L.; Vogel, J.M.; Topol, E.J. Long COVID: major findings, mechanisms and recommendations. *Nature Reviews Microbiology* **2023**, *21*, 133-146.
5. Nehme, M.; Chappuis, F.; Kaiser, L.; Assal, F.; Guessous, I. The prevalence, severity, and impact of post-COVID persistent fatigue, post-exertional malaise, and chronic fatigue syndrome. *Journal of General Internal Medicine* **2023**, *38*, 835-839.
6. Mueller, M.R.; Ganesh, R.; Hurt, R.T.; Beckman, T.J. Post-COVID conditions. In Proceedings of Mayo Clinic Proceedings; pp. 1071-1078.
7. Alonso-Domínguez, J.; Gallego-Rodríguez, M.; Martínez-Barros, I.; Calderón-Cruz, B.; Leiro-Fernández, V.; Pérez-González, A.; Poveda, E. High levels of IL-1β, TNF-$\alpha$ and MIP-1$\alpha$ one month after the onset of the acute SARS-CoV-2 infection, predictors of post COVID-19 in hospitalized patients. *Microorganisms* **2023**, *11*, 2396.
8. Patterson, B.K.; Francisco, E.B.; Yogendra, R.; Long, E.; Pise, A.; Rodrigues, H.; Herrera, M.; Hekmati, S.; Mora, J. Persistence of SARS CoV-2 S1 protein in CD16+ monocytes in post-acute sequelae of COVID-19 (PASC) up to 15 months post-infection. *Frontiers in immunology* **2022**, *12*, 746021.
9. Weidenbusch, M.; Anders, H.-J. Tissue microenvironments define and get reinforced by macrophage phenotypes in homeostasis or during inflammation, repair and fibrosis. *Journal of innate immunity* **2012**, *4*, 463-477.
10. Tang, J.; Xu, L.; Zeng, Y.; Gong, F. Effect of gut microbiota on LPS-induced acute lung injury by regulating the TLR4/NF-kB signaling pathway. *International immunopharmacology* **2021**, *91*, 107272.
11. Gao, L.-N.; Cui, Y.-L.; Wang, Q.-S.; Wang, S.-X. Amelioration of Danhong injection on the lipopolysaccharide-stimulated systemic acute inflammatory reaction via multi-target strategy. *Journal of ethnopharmacology* **2013**, *149*, 772-782.
12. Fernando, M.R.; Reyes, J.L.; Iannuzzi, J.; Leung, G.; McKay, D.M. The pro-inflammatory cytokine, interleukin-6, enhances the polarization of alternatively activated macrophages. *PloS one* **2014**, *9*, e94188.
13. Reis, P.A.; de Albuquerque, C.F.G.; Gutierrez, T.; Silva, A.R.; de Castro Faria Neto, H.C. Role of nitric oxide synthase in the function of the central nervous system under normal and infectious conditions. *Nitric Oxide Synthase–Simple Enzyme-Complex Roles. London: InTech* **2017**, 55-70.
14. Pahan, K.; Sheikh, F.G.; Namboodiri, A.; Singh, I. Lovastatin and phenylacetate inhibit the induction of nitric oxide synthase and cytokines in rat primary astrocytes, microglia, and macrophages. *The Journal of clinical investigation* **1997**, *100*, 2671-2679.
15. Rajakariar, R.; Yaqoob, M.M.; Gilroy, D.W. COX-2 in inflammation and resolution. *Molecular interventions* **2006**, *6*, 199.

 doi:10.20944/preprints202408.0306.v1




16. Al-Harbi, N.O.; Imam, F.; Al-Harbi, M.M.; Ansari, M.A.; Zoheir, K.M.; Korashy, H.M.; Sayed-Ahmed, M.M.; Attia, S.M.; Shabanah, O.A.; Ahmad, S.F. Dexamethasone attenuates LPS-induced acute lung injury through inhibition of NF-κB, COX-2, and pro-inflammatory mediators. *Immunological Investigations* **2016**, *45*, 349-369.
17. Millar, M.W.; Fazal, F.; Rahman, A. Therapeutic targeting of NF-κB in acute lung injury: A double-edged sword. *Cells* **2022**, *11*, 3317.
18. Moine, P.; McIntyre, R.; Schwartz, M.D.; Kaneko, D.; Shenkar, R.; Le Tulzo, Y.; Moore, E.E.; Abraham, E. NF-κB regulatory mechanisms in alveolar macrophages from patients with acute respiratory distress syndrome. *Shock* **2000**, *13*, 85-91.
19. Singleton, K.D.; Beckey, V.E.; Wischmeyer, P.E. Glutamine prevents activation of NF-κB and stress kinase pathways, attenuates inflammatory cytokine release, and prevents acute respiratory distress syndrome (ARDS) following sepsis. *Shock* **2005**, *24*, 583-589.
20. Tung, Y.-T.; Wei, C.-H.; Yen, C.-C.; Lee, P.-Y.; Ware, L.B.; Huang, H.-E.; Chen, W.; Chen, C.-M. Aspirin attenuates hyperoxia-induced acute respiratory distress syndrome (ARDS) by suppressing pulmonary inflammation via the NF-κB signaling pathway. *Frontiers in Pharmacology* **2022**, *12*, 793107.
21. Abraham, E. NF-κB activation. *Critical Care Medicine* **2000**, *28*, N100-N104.
22. Xin, W.; Zi-Yi, W.; Zheng, J.-H.; Shao, L. TCM network pharmacology: a new trend towards combining computational, experimental and clinical approaches. *Chinese journal of natural medicines* **2021**, *19*, 1-11.
23. Ru, J.; Li, P.; Wang, J.; Zhou, W.; Li, B.; Huang, C.; Li, P.; Guo, Z.; Tao, W.; Yang, Y. TCMSP: a database of systems pharmacology for drug discovery from herbal medicines. *Journal of cheminformatics* **2014**, *6*, 1-6.
24. Wang, Y. Network Pharmacology Approaches for Understanding Traditional Chinese Medicine. University of Helsinki, Finland, 2021.
25. Chun, S.-C.; Jee, S.Y.; Lee, S.G.; Park, S.J.; Lee, J.R.; Kim, S.C. Anti-inflammatory activity of the methanol extract of moutan cortex in LPS-activated Raw264. 7 cells. *Evidence-based Complementary and Alternative Medicine: eCAM* **2007**, *4*, 327.
26. Kim, H.M.; Nam, B.; Paudel, S.B.; Nam, J.-W.; Han, A.-R.; Jeong, H.G.; Jin, C.H. 9-Hydroxy-isoegomaketone inhibits LPS-induced NO and inflammatory cytokine production in RAW264. 7 cells. *Molecular Medicine Reports* **2021**, *23*, 1-1.
27. Xu, J.; Zhao, Y.; Aisa, H.A. Anti-inflammatory effect of pomegranate flower in lipopolysaccharide (LPS)-stimulated RAW264. 7 macrophages. *Pharmaceutical Biology* **2017**, *55*, 2095-2101.
28. Choi, W.-S.; Shin, P.-G.; Lee, J.-H.; Kim, G.-D. The regulatory effect of veratric acid on NO production in LPS-stimulated RAW264. 7 macrophage cells. *Cellular immunology* **2012**, *280*, 164-170.
29. Wu, C.; Zhao, W.; Zhang, X.; Chen, X. Neocryptotanshinone inhibits lipopolysaccharide-induced inflammation in RAW264. 7 macrophages by suppression of NF-κB and iNOS signaling pathways. *Acta Pharmaceutica Sinica B* **2015**, *5*, 323-329.
30. Guo, C.; Yang, L.; Luo, J.; Zhang, C.; Xia, Y.; Ma, T.; Kong, L. Sophoraflavanone G from Sophora alopecuroides inhibits lipopolysaccharide-induced inflammation in RAW264. 7 cells by targeting PI3K/Akt, JAK/STAT and Nrf2/HO-1 pathways. *International Immunopharmacology* **2016**, *38*, 349-356.
31. Kwon, O.-K.; Lee, M.-Y.; Yuk, J.-E.; Oh, S.-R.; Chin, Y.-W.; Lee, H.-K.; Ahn, K.-S. Anti-inflammatory effects of methanol extracts of the root of Lilium lancifolium on LPS-stimulated Raw264. 7 cells. *Journal of ethnopharmacology* **2010**, *130*, 28-34.
32. Greene, C.; Connolly, R.; Brennan, D.; Laffan, A.; O'Keeffe, E.; Zaporojan, L.; O'Callaghan, J.; Thomson, B.; Connolly, E.; Argue, R. Blood–brain barrier disruption and sustained systemic inflammation in individuals with long COVID-associated cognitive impairment. *Nature neuroscience* **2024**, *27*, 421-432.
33. Ran, J.; Li, H.; Fu, J.; Liu, L.; Xing, Y.; Li, X.; Shen, H.; Chen, Y.; Jiang, X.; Li, Y. Construction and analysis of the protein-protein interaction network related to essential hypertension. *BMC systems biology* **2013**, *7*, 1-12.
34. Bonnot, T.; Gillard, M.B.; Nagel, D.H. A simple protocol for informative visualization of enriched gene ontology terms. *Bio-protocol* **2019**, e3429-e3429.
35. Lim, D.W.; Ahn, J.Y.; Yu, G.R.; Kim, J.E.; Park, W.H.; Lim, D.W.; Ahn, J.Y.; Yu, G.R.; Kim, J.E.; Park, W.H. Study on the distribution in major disease category and frequency of clinical usage of national health insurance herbal prescription based on analysis on KCD8 disease code of indications. *Journal of Korean Medicine* **2023**, *44*, 1-15.
36. Tahaghoghi-Hajghorbani, S.; Zafari, P.; Masoumi, E.; Rajabinejad, M.; Jafari-Shakib, R.; Hasani, B.; Rafiei, A. The role of dysregulated immune responses in COVID-19 pathogenesis. *Virus research* **2020**, *290*, 198197.
37. Tecchio, C.; Cassatella, M.A. Neutrophil-derived cytokines involved in physiological and pathological angiogenesis. *Angiogenesis, Lymphangiogenesis and Clinical Implications* **2014**, *99*, 123-137.
38. Sun, S.-C.; Ganchi, P.A.; Ballard, D.W.; Greene, W.C. NF-κB controls expression of inhibitor IκBα: evidence for an inducible autoregulatory pathway. *Science* **1993**, *259*, 1912-1915.
39. Ratan, Z.A.; Haidere, M.F.; Hong, Y.H.; Park, S.H.; Lee, J.-O.; Lee, J.; Cho, J.Y. Pharmacological potential of ginseng and its major component ginsenosides. *Journal of ginseng research* **2021**, *45*, 199-210.

40. Christensen, L.P. Ginsenosides: chemistry, biosynthesis, analysis, and potential health effects. *Advances in food and nutrition research* **2008**, *55*, 1-99.
41. You, L.; Cha, S.; Kim, M.-Y.; Cho, J.Y. Ginsenosides are active ingredients in Panax ginseng with immunomodulatory properties from cellular to organismal levels. *Journal of ginseng research* **2022**, *46*, 711-721.
42. Shahrajabian, M.H.; Sun, W.; Cheng, Q. A review of ginseng species in different regions as a multipurpose herb in traditional Chinese medicine, modern herbology and pharmacological science. *Journal of Medicinal Plants Research* **2019**, *13*, 213-226.
43. He, M.T.; Park, G.; Park, D.H.; Choi, M.; Ku, S.; Go, S.H.; Lee, Y.G.; Song, S.J.; Ahn, C.-W.; Jang, Y.P. So Shiho Tang Reduces Inflammation in Lipopolysaccharide-Induced RAW 264.7 Macrophages and Dextran Sodium Sulfate-Induced Colitis Mice. *Biomolecules* **2024**, *14*, 451.
44. Ohtake, N.; Nakai, Y.; Yamamoto, M.; Sakakibara, I.; Takeda, S.; Amagaya, S.; Aburada, M. Separation and isolation methods for analysis of the active principles of Sho-saiko-to (SST) oriental medicine. *Journal of Chromatography B* **2004**, *812*, 135-148.
45. Tran, N.K.S.; Lee, J.H.; Lee, M.J.; Park, J.Y.; Kang, K.S. Multitargeted Herbal Prescription So Shiho Tang: A Scoping Review on Biomarkers for the Evaluation of Therapeutic Effects. *Pharmaceuticals* **2023**, *16*, 1371.
46. Kang, B.-h.; Choi, Y.-k.; Jeon, C.-y.; Yang, S.-b. The effects of Qingfei Paidu Decoction on coronavirus disease-19: A narrative review. *The Journal of Internal Korean Medicine* **2020**, *41*, 424-433.
47. Lim, D.-W.; Kim, D.-H.; Yu, G.-R.; Park, W.-H.; Kim, J.-E. Verification of the Potential Targets of the Herbal Prescription Sochehwan for Drug Repurposing Processes as Deduced by Network Pharmacology. *Processes* **2021**, *9*, 2034.
48. Kim, T.-H.; Yu, G.-R.; Kim, H.; Kim, J.-E.; Lim, D.-W.; Park, W.-H. Network pharmacological analysis of a new herbal combination targeting hyperlipidemia and efficacy validation in vitro. *Current Issues in Molecular Biology* **2023**, *45*, 1314-1332.